



Experimental Study of Flow Patterns and Pressure Drop Reduction in Pipes of Oil-Water Flow

دراسة عملية لأنماط التدفق والتخفيض في فقد الضغط في الأنابيب لسريان زيت - ماء

R.G. Abd Elkhalek, M. M. Awad and L. H. Rabie

KEYWORDS:

Oil-water; Flow pattern; Stratified; Core-annular; Pressure drop reduction

المخلص العربي:- الزيوت الثقيلة لا يمكن أن تتدفق بسهولة في الأنابيب نظراً لزوجةها العالية ، ومن ثم هناك حاجة إلى تكنولوجيا لتحسين نقل وإنتاج هذه الزيوت. نقل الزيوت الثقيلة باستخدام الماء كوسيط تزييت بين الزيت الثقيل وجدار الأنبوب الداخلي تبدو طريقة فعالة في تقليل القدرة المستهلكة في عمليات النقل. في هذه الدراسة، تم عملياً دراسة تأثير تغيير سرعة الماء عند بدايه الحقن لنفس معدل سريان الماء على أشكال أنماط السريان والفقء في الضغط باستخدام زيت ثقيل ذات لزوجة (750 mPa.s عند 40 درجة مئوية) في انبوبة افقية بطول 3.66 متر كطول اختبار وقطر داخلي 29مم تم التعرف على ستة أنماط تدفق مختلفة بمساعدة التصوير الفوتوغرافي وتم إنشاء خرائط أنماط التدفق لكل حالة. معامل التخفيض في فقد الضغط أستخدم لتوصيف السريان الثنائي الطور(زيت-ماء). من النتائج العملية لوحظ أنه بزيادة كمية الزيت المنقولة أى في اتجاه تكوين السريان الحلقي يزداد معامل التخفيض في فقد الضغط ونقل كمية الماء المحقونة. تم مقارنة النتائج العملية لمعامل التخفيض في فقد الضغط مع الحل التحليلي لنموذج (Arney). من المقارنة كانت نسبة الحيوء بين النتائج العملية لهذه الدراسة ونتائج النموذج الرياضي أقل من 20%.

Abstract— Heavy oils cannot easily flow through pipes due to their high viscosity. Technologies to enhance the mobility of heavy oils are required in oil production and transportation. Transportation of heavy oil by lubricated technique looks an attractive method for saving pumping power. In this study, the effect of varying mean injection velocity of water on the flow structure and the pressure gradient of the two-phase flow was studied experimentally by using heavy oil (viscosity = 750 mPa.s at 40 °C) flow in a horizontal pipe of 29 mm inner diameter and 3.66 m long test section. With the help of photography, six different flow patterns were identified and the flow pattern maps

were constructed for each case. The pressure drop reduction factor was introduced to characterize the oil-water two-phase flow. From the results, the pressure drop reduction factor increases with increasing the amount of oil transported.

The water input ratio decreases with increasing the oil flow rate (in the direction of annular flow observation). The experimental data for pressure drop was compared with the analytical solution of Arney model. From the comparison, the deviation between the experimental data and the predication of the analytical model is less than 20%.

NOMENCLATURE

A_p	Main pipe cross section area, m^2	J	Superficial velocity, m/s
		l	Test section length, m
C_w	Water input ratio	R	Pressure drop reduction factor
D	Main pipe diameter, m	Re	Reynolds number
f	Friction factor	U	Injection velocity, m/s
H_w	Holdup volume fraction		

GREEK SYMBOLS

α	Water- diameter ratio at injection	ρ	Fluid density, kg/m^3
$\Delta P/l$	Pressure gradient, Pa/m	ϕ	Dimensionless pressure drop (1/R)
η	Core-diameter ratio	μ	Fluid dynamic viscosity, Pa.s

Received: 1 November, 2017 - accepted: 21 February, 2018

R.G. Abd Elkhalek is with the Mechanical Power Engineering Department, Faculty of Engineering, Mansoura University, Egypt (e-mail: engramadagad@mans.edu.eg).

M.M. Awad is with the Mechanical Power Engineering Department, Faculty of Engineering, Mansoura University, Egypt (e-mail: m_m_awad@mans.edu.eg).

L.H. Rabie is with the Mechanical Power Engineering Department, Faculty of Engineering, Mansoura University, Egypt (e-mail: lotfyr@mans.edu.eg).

SUBSCRIPTS

m	Mixture	o	Oil
max	Maximum	w	Water
min	Minimum		

ABBREVIATIONS

A	Annular flow (oil in the core)
A _w	Annular flow (water in the core)
B	Bubbly flow
C	Churn flow
CAF	Core-annular flow
DC	Dual continuous
D _{o/w}	Dispersion oil in water phase
D _{w/o}	Dispersion water in oil phase
D _{o/w&o}	Dispersion oil in water and oil film
D _{o/w&w}	Dispersion oil in water and water layer
D _{w/o&E}	Dispersion water in oil and emulsion
P	Plug flow
P _w	Water plug in oil phase
S	Slug flow
SD-SE&TO	Semi dispersion with semi emulsion at interface and thin film oil
SM	Stratified mixed flow
SS	Smooth stratified flow
SW-SD&O	Stratified wavy with semi dispersion at interface and oil film
SW	Stratified wavy flow
S _w	Water slug in oil phase
SW&OI	Stratified wavy with oil droplets at interface
TL	Three layer flow
WCAF	Wavy core-annular flow

INTRODUCTION

NOWADAYS oils represent the most important source of energy utilized all over the world. So, the demand for light oil increased so much that the reserves for light oils are getting dangerously low.

This has pushed engineers and scientists to think of heavy oil as a suitable alternative to conventional oil.

Heavy oils are characterized by high viscosity. So the pressure drop in the pipes is very high, resulting in high pumping cost. Because of this, the pressure drop must be minimized to decrease the pumping power required to drive the heavy oil over long distance to make its transportation economical. Technologies to enhance the mobility of heavy oils are required in oil production and transportation, these methods are summarized in Fig.1.

Some of these methods were used to reduce the oil viscosity (viscosity reduction) such as dilution or blending; in this method, viscosity of heavy oil is reduced by using less viscous diluents resulting in a less viscous blending mixture.

Another way to reduce oil viscosity is the heating. Heating has a great effect on viscosity reduction. Decreasing the temperature of heavy oils results in reducing its viscosity. One of the newest methods of heavy oil transporting is emulsion of heavy oil with water. In this technique, oil droplets are

dispersed in the water phase and become stable by the aid of a suitable surfactant, resulting in a reduction in emulsion viscosity.

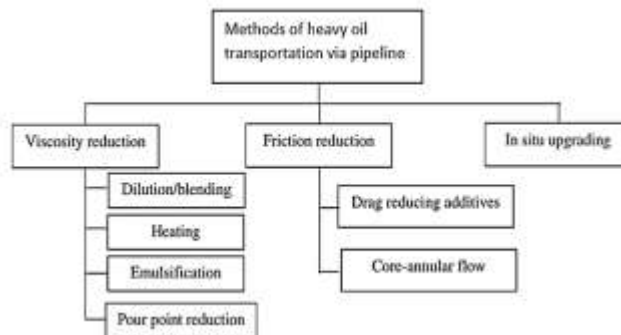


Fig.1. Methods of heavy oil transportation Gateau et al. [1]

Transferring waxy crude oil in cold weather is so difficult, so pour point depression is an attractive method to minimize the wax by adding copolymers.

The other branch for transport heavy oils is friction reduction. One of these methods is drag-reduction-additives. This is a promising technique for pipeline transportation, where these additives reduce wall friction and turbulence of the core fluid. Toms [2] shows that about 30 – 40% drag reduction was generated by adding a polymer to flow.

The second method for friction reduction is water lubricating, where a small amount of water is introduced in the flow of oil and act as a lubricant. The most effective configuration incorporates oil in the core surrounded by a thin layer of water near the wall so that the pumping pressure is the pump required to transfer the water. Saniere et al. [3] found that the required amount of water varies from 10 to 30%.

In-Situ upgrading; the viscosity of oil reservoir is reduced by heating to improve its flow from production well.

Limitations for using some of the pervious methods are such as the cost of the external additives, problem of stability and separation of the additives. Weather may limit the use of some of these methods, such as heating.

The lubricating technique has advantages over other methods for the following reasons; the lubricated fluid is inexpensive, oil does not go emulsion in water, no external additives are required to stabilize the flow and no attention to material pipe, where the oil does not contact with the pipe wall. So, this technique is selected over other methods.

In multiphase flow, many different flow patterns exist, ranging from stratified flow where two layers exist to dispersed flow with small droplets dispersed in other continuous phase. Other flow patterns exist in multiphase flow such as plug/slug flow which appear when the velocity of low fluid flow rate was increase. The best option for pressure drop reduction is core-annular flow. Many parameters have a great effect on flow pattern such as density and viscosity of oil, pipe diameter, surface tension and the shear rate in the flow. Mean

injection velocities are also key parameters for the flow regime determination, Bensakhria et al. [4].

Table 1 summarizes the flow patterns of oil–water flow in horizontal pipe. Annular flow was not observed in many studies (Dasari et al. [5], Angeli and Hewitt [6], Lovick and Angeli [7], Ismail et al. [8] and Vuong et al. [9]) due to problems of mixing of two phases. Annular flow was observed in using heavy and light oils (Sotgia et al. [10], Poesio et al. [11], Grassi et al. [12] and Hanafizadeh et al. [13]). In case of using matched density of two-phase, the core flow may be water in oil (Charles et al. [14] and Fujii et al. [15]).

Table 1
Summarized flow patterns of oil–water flow in horizontal pipe

Authors	μ_o/μ_w	ρ_o/ρ_w	Pipe ID (cm)	Pattern observed
Dasari et al. [5]	107	0.889	2.5	S, P, SW, SM, $D_{o/w}$, $D_{w/o}$
Angeli and Hewitt [6]	1.6	0.801	2.5	SW, TL, SM, $D_{o/w}$, $D_{w/o}$
Lovick and Angeli [7]	6	0.828	3.8	DC, $D_{o/w\&w}$, $D_{w/o}$, $D_{o/w}$
Ismail et al. [8]	1.75	0.818	5.08	SW, SW-SD&O, SD-SE&TO, $D_{w/o\&E}$, $D_{o/w}$
Vuong et al. [9]	225	0.884	5.25	SW&OI, $D_{o/w\&w}$, $D_{o/w}$, $D_{o/w\&o}$
Sotgia et al. [10]	900	0.9	21 : 40	$D_{o/w}$, A, S, SW
Poesio et al. [11]	900	0.89	5	$D_{o/w}$, B, A
Grassi et al. [12]	799	0.886	2.1	SS, SW, P, S, A, $D_{o/w}$
Hanafizadeh et al. [13]	4.5	0.84	2	B, S, SS, SW, C, A, DC
Charles et al. [14]	16.8	0.998	2.54	$D_{w/o}$, A, S, P, $D_{o/w}$
Fujii et al. [15]	16.8	0.998	2.54	$D_{w/o}$, A, A_w , S, S_w , P_w , P, $D_{o/w}$

One of the first works on annular flow was studied by Abraham and Clark [16] for traveling high viscous oil through the pipe. They reported that by adding of 24% of water, it reduces the pressure gradient by factor 7.8 to 10.5, but no details were reported about flow pattern. More details for core flow such that flow regimes, flow map, holdup ratio pressure gradient are obtained by Charles et al. [14] and Fujii et al. [15] experimental studies using oil and water of matched density.

Experimental studies validated with theoretical model of using two different pipe diameters and different oil viscosities are investigated by Ooms et al. [17] and Miesen et al. [18]. The effect of pipe diameter on pressure drop for core-annular flow was studied and a mathematical model based on two fluid Poiseuille flow to predict the interfacial waves was developed.

More details about pressure gradient, amplitude and length

of the waves, film thickness and water hold up were carried out by Oliemans et al. [19]

Arney et al. [20] and Beretta et al. [21] carried out experimental studies using different oil viscosities. The pressure gradient and the holdup are measured with different flow rate ratio and their results compared with other literature and suggested an empirical correlation for holdup in terms of input water fraction.

Bensakhria et al. [4] carried out an experimental study of heavy oil of viscosity equal 4.74 Pa.s. From experiments, they reported that for a fixed oil flow rate, the maximum reduction of 90% in pressure drop for the annular flow rate at water-oil ratio of 6%.

The effect of pipe inclination in the observed flow patterns, the flow pattern map and the pressure drop is carried out by Grassi et al. [12]. They reported that the slight variation in the pipe inclination angle has no effect on the previous parameter. Pressure drop measured experimentally were compared to empirical relations obtained by Brauner and Ullmann [22] and show good agreement around 20% accuracy.

The influence of connecting shape between the inlet mixer to the pipe on observed flow pattern and pressure drop was studied by Sotgia et al. [10]. A set of different pipes is used, where R_{max} is independent of the pipe diameter and material for J_o less than 0.8, but for more than 0.8, the maximum water input ratio is constant and about 10%. The measured pressure drop was compared with empirical relations obtained by Brauner [23] and Arney et al. [20].

Heavy and light oil-water two-phase flows were experimentally studied by Loh and Premanadhan [24]. The pressure drop behavior of two oil-water combinations was investigated. They constructed the flow pattern map and compared the observed flow pattern of the two oils.

An experimental study of the flow structure and the pressure gradient of extra-heavy oil-water two-phase flow is carried out by Luo et al. [25]. A new flow pattern discrete water in oil emulsion and dispersion annular flow was found. The effect of water fraction and temperature on pressure gradient of oil dominate and water dominate was studied.

Models of core flow study many parameters like the effect of operating condition on the shape of core flow (shape and amplitude of the wave and eccentricity), predication correlation relation for pressure gradient, hold up and radial velocity. These models vary from laminar to turbulent one.

Huang et al. [26] studied the numerical modeling of eccentric core-annular to show the effect of the eccentricity and the volume flow rate on the holdup ratio and the friction factor.

Most models were investigated to obtain velocity profiles, interfacial and wall shear stress, and hold up, pressure drop and power reduction of CAF (Rovinsky et al. [27] and Ko et al. [28]).

Simulation of wavy and eccentric core-annular flow by solving the Navier-Stokes equation with taking the turbulence in the annulus into account and comparison with the experimental data for pressure drop and interfacial wave were investigated by Ingen Housz et al. [29].

CFD simulation of a matched density oil-water two-phase flow of medium viscosity for different flow regimes were performed by Shi et al. [30]. The effect of the turbulence and the wall contact angle were investigated for CAF and compared with the experimental results.

The previously mentioned reviews extensively the effects of different parameters (density ratio, viscosity ratio, pipe diameter, shape of connection between injector and main pipe and inclination angle) on the flow pattern observations, the flow pattern maps and the pressure drop in addition to the models that predict pressure gradient, hold up, velocity profile and transfer from pattern to another.

There are not enough details about the effect of variation of the mean injection water velocity on the flow patterns observation, the flow pattern map and the pressure drop.

In the present study, the effect of varying the injection water velocity for the same water flow rate on the flow patterns observation, the flow pattern maps and the pressure drop is investigated. Also, the effect of using lubricating method as a technique for transporting heavy oils is studied.

II. EXPERIMENTAL WORK

The experimental test rig has been constructed in

Hydraulic Machines Laboratory (Mechanical Power Engineering Department) of the Faculty of Engineering, Mansoura University to investigate the drag reduction based on the core annular flow of heavy oil lubricated by water. The system consists of a flow loop, Fig. 2, containing acrylic pipe of total length of 10 m and inner diameter of 29 mm with test section of 3.66 m long. This type of pipe (acrylic pipe) is used to easily identify the different flow regimes by visual observation and record it by taking a photo.

The heavy oil is stored in a tank of 150 liters capacity and transferred using a positive displacement pump (vane pump of power 4 hp) to the center of the injector located at the head of the pipe. Water is pumped to injector section by using two centrifugal pumps of 1 hp of each with two water tanks of capacity of 75 liters.

The oil flow rate is measured by weighting method and water flow rate is measured by using an orifice meter. The pressure drops within the pipeline is measured using an inverted air manometer. The pressure tap was installed 3 m from injection section ($L/D = 105$) for fully developed flow.

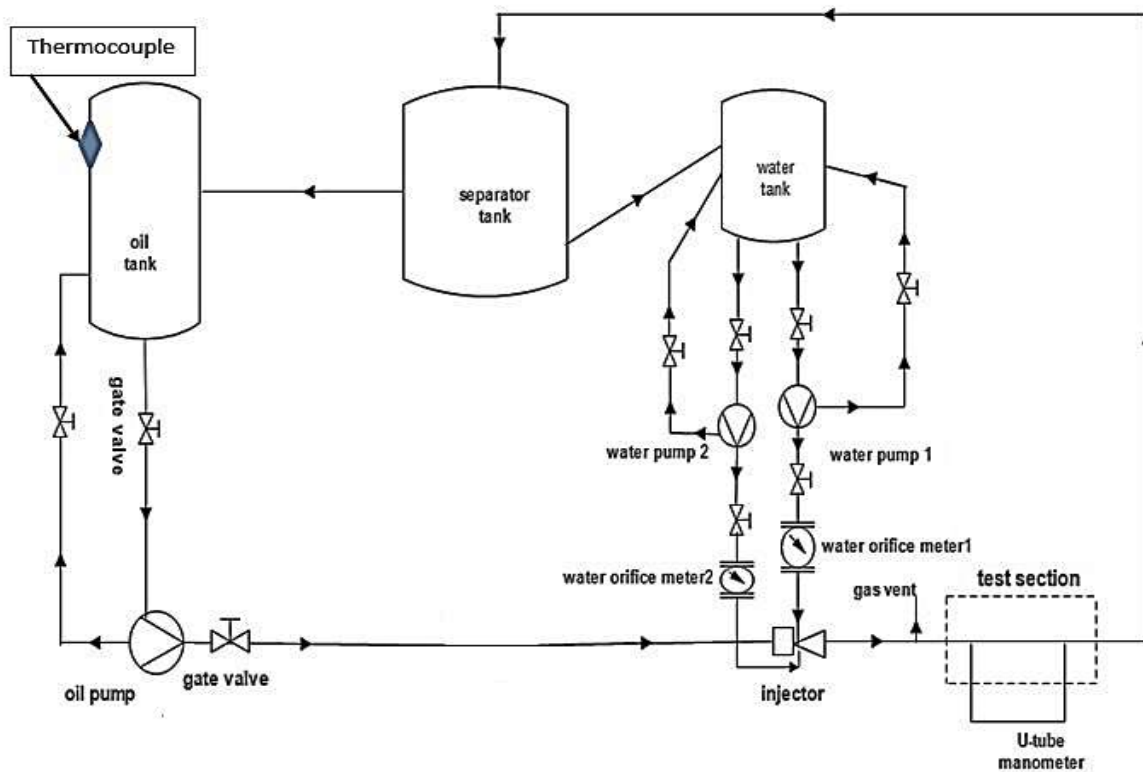


Fig. 2. Schematic diagram of the experimental test rig

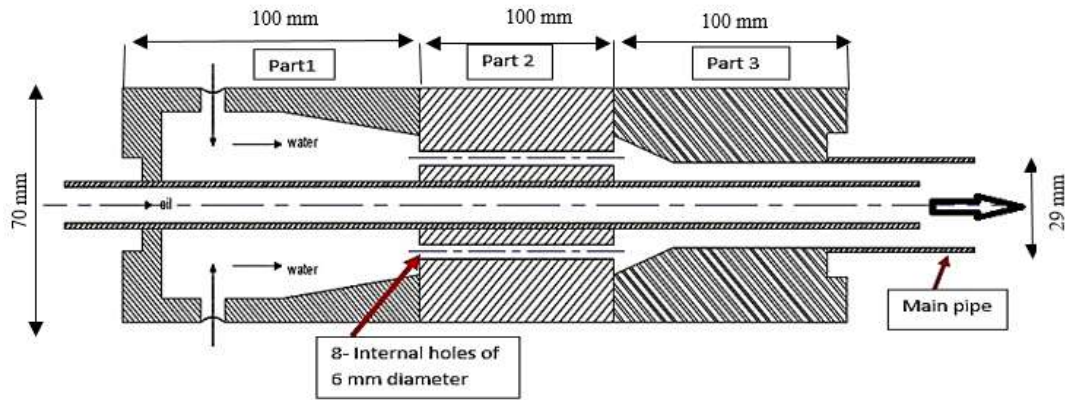


Fig. 3. Schematic diagram of the fluid injector

Figure 3 shows a schematic diagram of the desired design of nozzle (fluid injector) for establishing the core-annular flow. In this design, the injector consists of three parts. The lubricating fluid is injected from two slots to the annulus where it is reduced gradually (Part 1) to the cylindrical section (Part 2). This section has a length of 10 cm and contains eight holes of 6 mm inner diameter surrounding the passage of oil to suppressing turbulence in Part 1 and makes the water enter into the third part without turbulence and tangent to the inner diameter of third section which has the same diameter of the main pipe to avoid turbulent flow and air bubbles at the beginning of injection.

Figure 4 shows the details of the second part with internal holes. The most affecting parameter in establishing the core flow is injection part so this part must be designed carefully. Many researchers mention that one of the reasons that core flow is not established is due to the design of injection section that cause oil and water to mix at the beginning of injection, Angeli and Hewitt [6] and Dasari et al. [5].



Fig. 4. Turbulence suppression section

Table 2

Fluid properties used in the experiments

Fluid	Density (kg/m ³)	Viscosity (m Pa.s)
Oil	900	750 (at 40 °C)
Water	1000	1

Vertical lines are optional in tables. Statements that serve as captions for the entire table do not need footnote letters.
^aGaussian units are the same as cg emu for magnetostatics; Mx = maxwell, G = gauss, Oe = oersted; Wb = weber, V = volt, s = second, T = tesla, m = meter, A = ampere, J = joule, kg = kilogram, H = henry.

The heavy oil used in experiments is base oils from Misr of Petroleum Company, Egypt, the properties of the two fluids used in the experiments are given in Table (2).

III. GOVERNING EQUATIONS

The superficial velocity J (m/s) which is defined as the volumetric flow rate of one single phase divided by the main pipe cross-section area

$$J_o = \frac{Q_o}{A_p} \quad \text{For oil phase} \quad (1)$$

$$J_w = \frac{Q_w}{A_p} \quad \text{For water phase} \quad (2)$$

The mixture superficial velocity is equal to the sum of two-phase superficial velocity

$$J_m = J_o + J_w \quad (3)$$

In order to show the effect of lubricating, the pressure drop reduction factor is defined as:

$$R = \frac{\frac{\Delta P_o}{l}}{\Delta P_m} \quad (4)$$

where $\frac{\Delta P_m}{l}$ is the measured pressure gradient of oil and water mixture flow in the pipe while $\frac{\Delta P_o}{l}$ is the pressure

gradient calculated using Hagen-Poiseuille law of laminar flow of oil have the same flow rate as the oil phase in the two-phase case.

$$\frac{\Delta P_o}{l} = \frac{32 \mu_o J_o}{D^2} \quad (5)$$

The water input ratio is defined as:

$$C_w = \frac{J_w}{J_m} \quad (6)$$

IV. EXPERIMENTAL PROCEDURE

The experimental procedure is carried out in the following steps:

- (1) Oil superficial velocity (J_o) is selected.
- (2) The experiment is started introducing only water, for J_w ,
_{max.}
- (3) Oil is introduced at the selected flow rate (J_o).
- (4) The water superficial velocity is decreased where water superficial velocity is changed from J_w ,_{max} to J_w ,_{min}.
- (5) In each step, the pressure drop is measured for the same J_o and various J_w and observed flow pattern at each J_w .
- (6) After each run the pipeline is cleaned to reduce the effect of oil fouling.

V. RESULTS AND DISCUSSION

Two sets of results are presented for the effect of varying the mean injection water velocity for the same water flow rate. The first set of results identifies the different observed flow patterns and constructs the flow pattern maps. The second set of results aims to measure the pressure drop of different flow regimes and study the effect of lubricating on the pressure drop reduction.

A. Flow Pattern Observations

One of the parameters that has a great effect on the flow pattern is the mean injection velocity of water at the beginning of injection (U_w). The effect of the change of U_w , while mean injection oil velocity remains constant on the flow pattern observation and the flow pattern map is discussed. To change U_w , the area in which water is injected is varied. This is occurred by changing the water diameter ratio (α), which is defined as the ratio of the outer diameter of the oil pipe to the inner diameter of the main pipe at injection.

1) Case 1 ($\alpha_1 = 0.88$)

Figures 5 and 6 show the dominant flow patterns observed in the smallest annulus area of water injection. Five main flow patterns were observed, dispersion oil in water, Plug, Slug, Eccentric annular flow with oil dispersion in water at interface and wavy annular flow. For each pictorial view series, the observed flow patterns appear when the oil flow rate is held constant and water flow rate is changed from maximum to minimum value.

Figure 5 shows the observed flow pattern of a relatively small superficial oil velocity ($J_o = 0.148$ m/s). Dispersion oil in water appears at high J_w where $J_w = 0.89$ m/s. By decreasing

J_w , the oil flows in the form of a plug flow (large bubbles). With further decrease in J_w , the bubbles become longer to form a slug flow at $J_w = 0.32$ m/s.

Figure 6 shows a clear picture of annular flow at high oil superficial velocity ($J_o = 0.35$ m/s). The flow pattern changes from dispersion of oil in water as shown in Fig. 6.a to annular pattern by decreasing J_w from 1 m/s to 0.44 m/s as shown in Fig. 6.b with oil dispersed in water at the interface. The annular flow become wavy as displaced in Fig. 6.c at low water superficial velocity ($J_w = 0.2$ m/s). Stratified flow does not appear in this case.

2) Case 2 ($\alpha_2 = 0.79$)

In the present case the water mean velocity at the injection is lowered by increasing the annular area of the water flow at the injection. Seven flow patterns were observed, dispersion oil in water, plug flow, slug flow, smooth and wavy stratified flow, eccentric core-annular flow and wavy core-annular flow. Fig. 7 shows the flow observed at low oil flow rate ($J_o = 0.146$ m/s), where the flow is changed from slug flow at high water flow rate to wavy stratified at low water flow rate. The annular flow was observed at high oil flow rate ($J_o \geq 0.2$ m/s) with smooth interface between oil and water.

3) Case 3 ($\alpha_3 = 0.72$)

This case represents the smallest water injection velocity. Seven flow patterns are observed like Case 2. The range of dispersed oil in water is very limited. Fig. 8 shows the observed flow pattern at very low superficial oil velocity ($J_o = 0.035$ m/s). The plug flow pattern was observed at very low J_o as shown in Fig. 8.b. CAF appears at high J_o , where the eccentric core-annular appear at J_w ,_{max} to J_w ,_{min}. At the beginning of injection, the formed CAF is concentric but after a long distance, the buoyancy force pushes it up, but the oil doesn't touch the pipe wall as shown in Fig. 9.

B. Flow Pattern Map

Flow pattern maps were investigated for the three cases discussed before and depicted as shown in Figs. 10-12. The flow map is a map used to indicate the region of various patterns and the velocity boundaries at which the phase inverse takes place as a function of oil and water superficial velocity.

From Case 1, where U_w is high as compared to Cases 2 and 3 and have the same core diameter ratio. The dispersion of oil in water exists in the three cases, but in Case 1 it exists in a wide range of operation for the same water flow rate in the three cases. In Cases 2 and 3, the dispersion flow has a narrow range especially in Case 3.

Stratified flow exists at relative low oil and water superficial velocities. This type of flow does not appear in Case 1, but it occurs in a limited range of operation in Cases 2 and 3, where U_w was decreased.

The core-annular flow exists in a wide range of operation of oil and water flow. This type of flow pattern appears at high oil superficial velocity in the three cases. In Case 1, the appeared CAF is eccentric with oil dispersion in water at the interface at relatively high oil and water superficial velocities, but in Case 2 and Case 3, smooth CAF flow exists at a wider

range than Case 1. At very low J_w , wavy CAF is dominated in the three cases.

C. Pressure Drop Calculation

The measured pressure gradient is plotted as a function of the water input ratio (C_w) as shown in Figs. 13-14. In these figures, the different lines refer to the different oil superficial velocities and different symbols indicate the different flow regimes. From the analysis, the pressure drop decreases in direction of core-annular flow and with decreasing the water input ratio. The trend line of each superficial of oil velocity of core flow and some other patterns show that the heavy oil can be transferred with pressure drop as the water flows only at the same mixture velocity as shown in Fig. 15.

All attempts to obtain annular flow, where pressure drop is less compared to other flow patterns at the same oil flow rate as shown in Fig. 16.

D. Reduction Factor Calculation

When the heavy oil is transported in the form of annular flow pattern and water flow rate is reduced, the pressure gradient starts to decrease resulting in an increase in the reduction factor (R) until it reaches to a maximum value at high J_o and low water fraction as shown in Figs. 17-18.

Since the procedure of experiments was conducted firstly with high water fraction and in the direction of decreasing the water flow rate, therefore, the plots of this section should be read from right to left.

The maximum pressure drop reduction factor R_{max} as a function of the oil flow rate is plotted in Fig. 19. for the three cases. From this figure, the value of R_{max} increases with increasing the oil flow rate where the core-annular flow regimes exist. Also, the water input ratio (C_w) corresponding to R_{max} as a function of the oil superficial velocity is shown in Fig. 20. From the figure, C_w for R_{max} decreases with the increase of the oil flow rate; this means that heavy oil can be transferred with high reduction in pressure drop using a small amount of water.

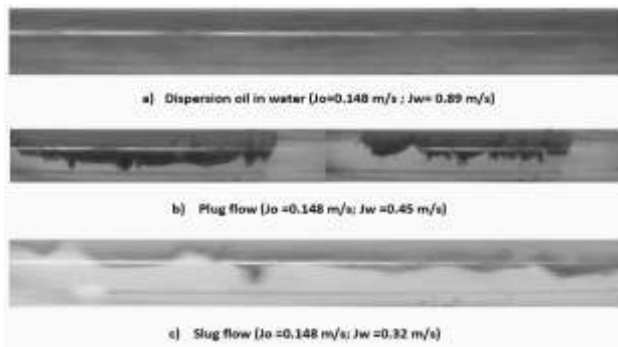


Fig. 5. Flow pattern observed for $J_o = 0.148$ m/s for Case 1

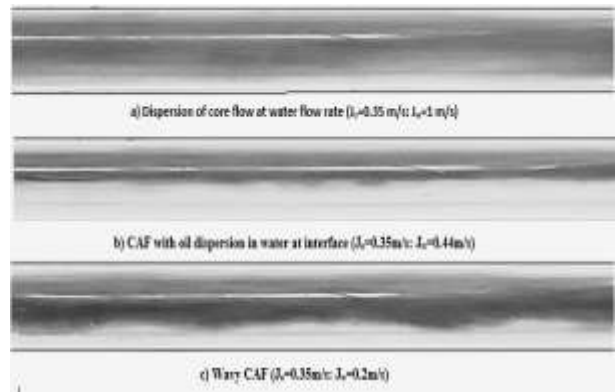


Fig. 6. Flow pattern observed for $J_o = 0.35$ m/s for Case 1

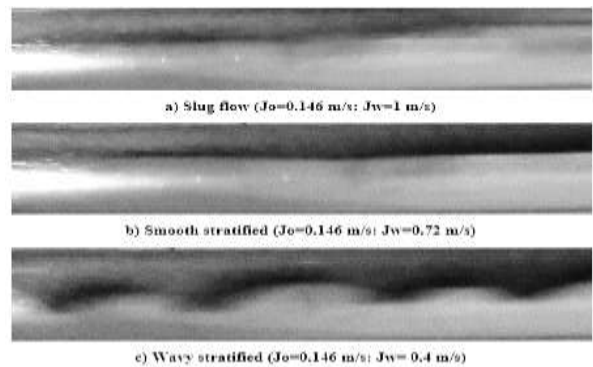


Fig. 7. Flow pattern observed at $J_o = 0.146$ m/s for Case 2

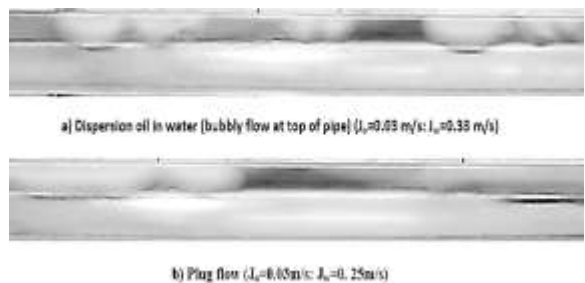


Fig. 8. Flow pattern observed for $J_o = 0.03$ m/s for Case 3

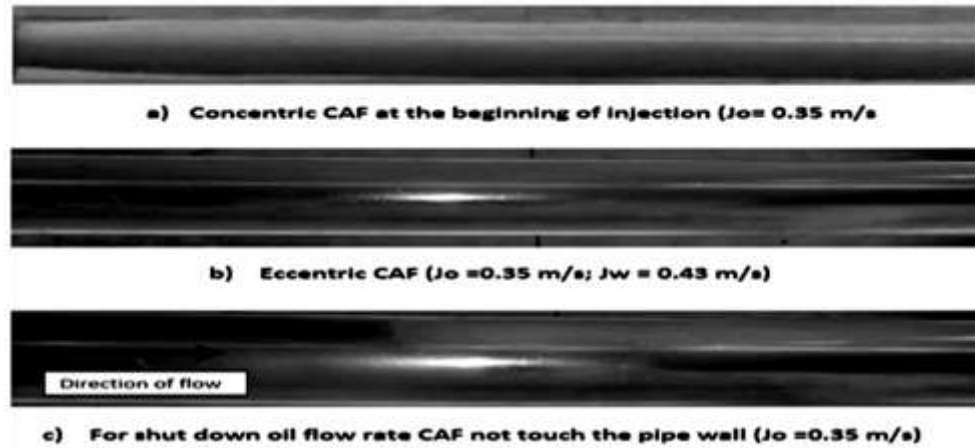


Fig.9. Flow pattern observed for $J_o = 0.35 \text{ m/s}$ for Case 2

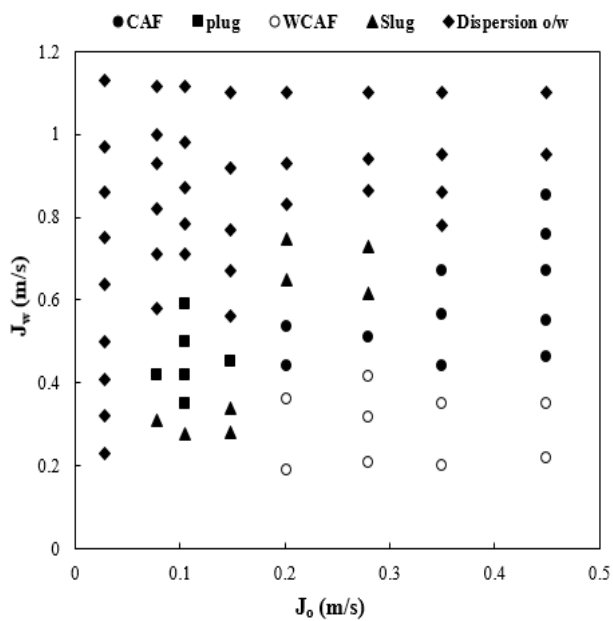


Fig. 10. Flow pattern map for Case 1

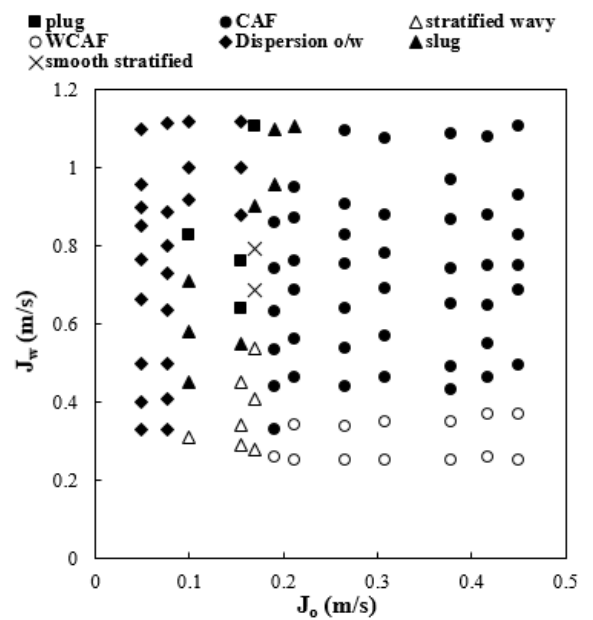


Fig. 11. Flow pattern map for Case 2

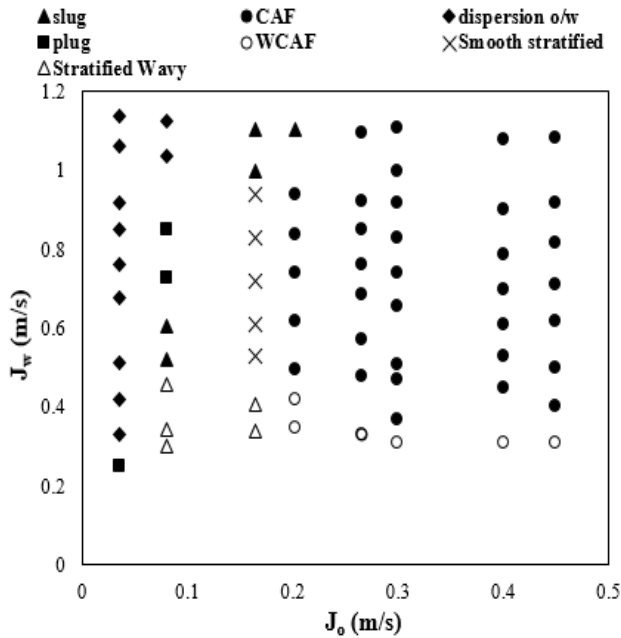


Fig. 12. Flow pattern map for Case 3

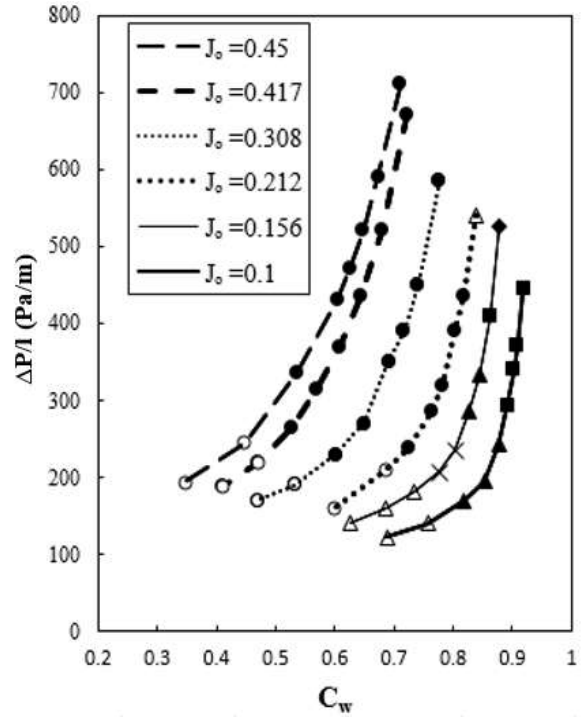


Fig. 14. Measured pressure gradients as function of input water ratio (Case 2)

\blacklozenge =dispersion oil in water; \blacksquare =plug; \blacktriangle =slug; \triangle =stratified wavy; \times = smooth stratified; \bullet =core-annular; \circ =wavy annular

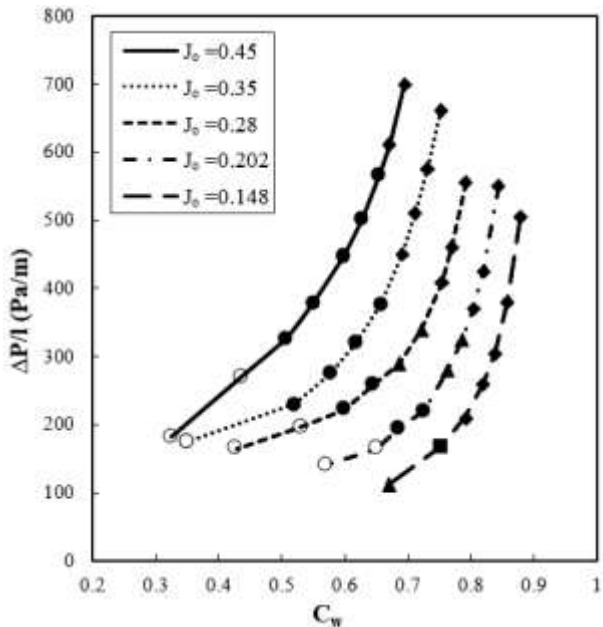


Fig. 13. Measured pressure gradient as function of input water ratio (Case 1)

\blacklozenge =dispersion oil in water; \blacksquare =plug; \blacktriangle =slug; \bullet =core-annular; \circ =wavy annular

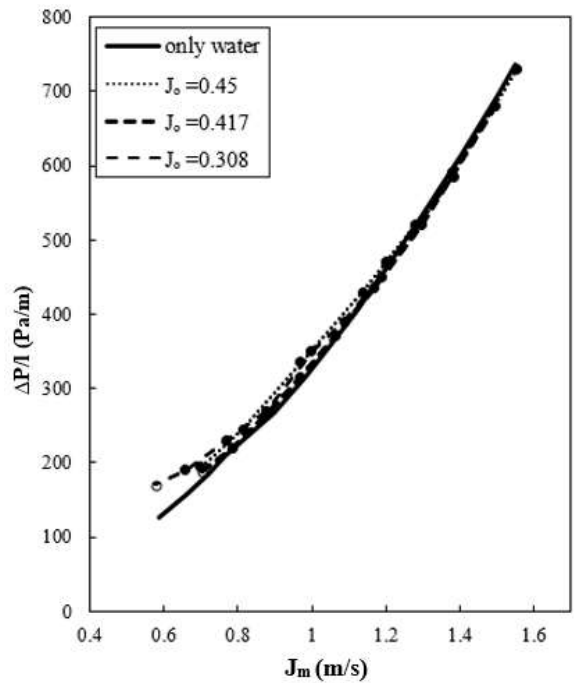


Fig. 15. Pressure gradients as function of mixture velocity compared with only water; \bullet =core-annular; \circ =wavy core-annular; solid line represents pressure drop for only water.

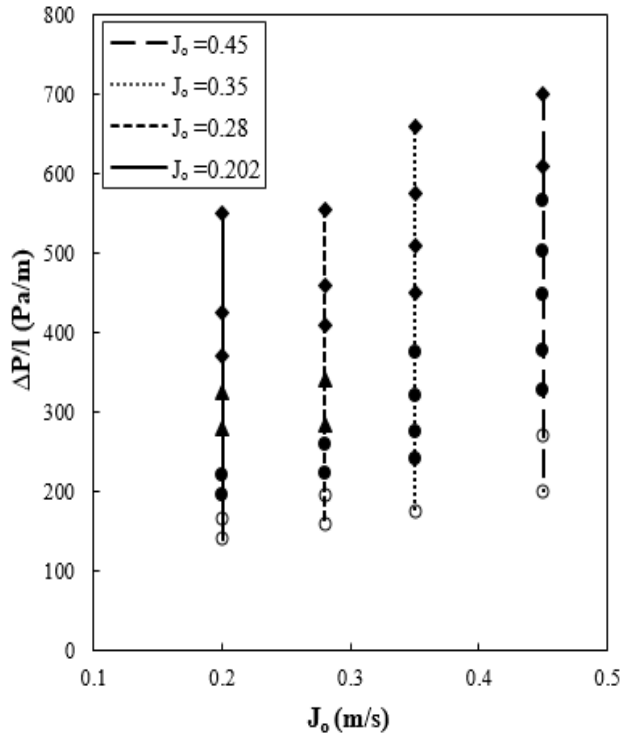


Fig. 16. Pressure gradient as function of superficial oil velocity ◆=dispersion oil in water; ■=plug; ▲=slug; ●=core-annular; ○=wavy core-annular

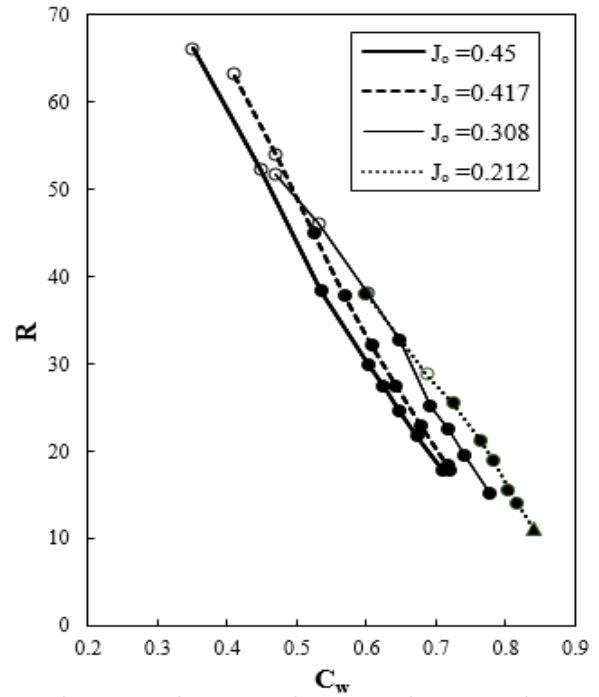


Fig. 18. Pressure drop reduction factor (R) as function of water input ratio (C_w) for Case 2
◆=dispersion oil in water; ■=plug; ▲=slug; ●=core-annular; ○=wavy core-annular.

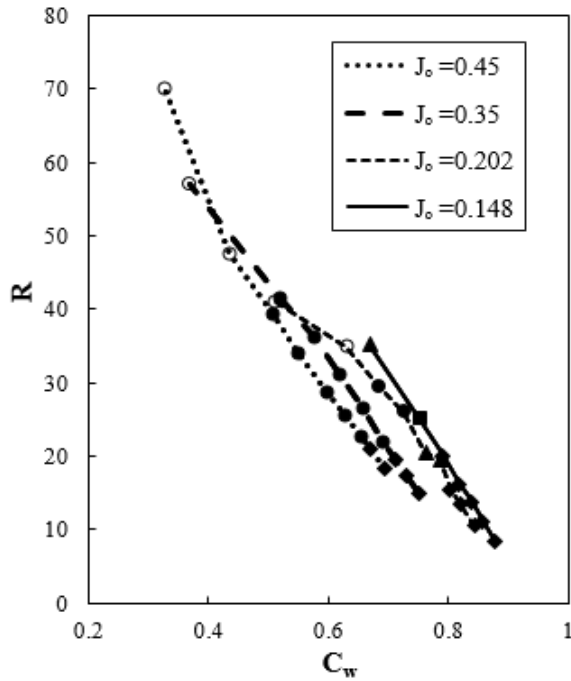


Fig. 17. Pressure drop reduction factor (R) as function of water input ratio (C_w) for Case 1
◆=dispersion oil in water; ■=plug; ▲=slug; ●=core-annular; ○=wavy core-annular.

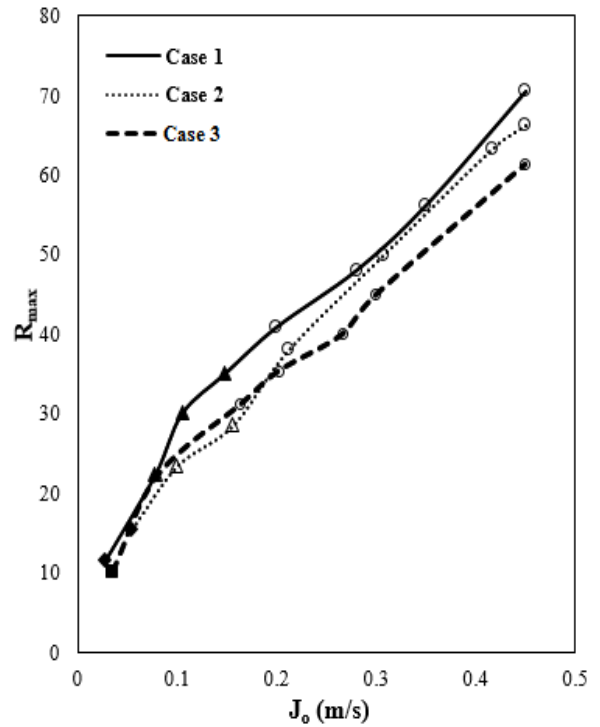


Fig. 19. Maximum pressure drop reduction factor as function of superficial velocity of oil; ◆=dispersion oil in water; ■=plug; ▲=slug; △=wavy stratified; ●=core-annular; ○=wavy annular.

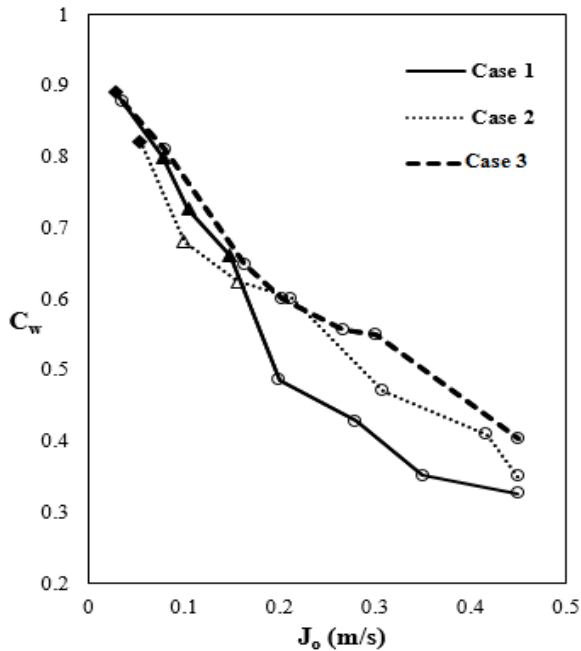


Fig. 20. Maximum water input ratio corresponding to R_{max} as function of oil flow rate; \blacklozenge =dispersion oil in water; \blacksquare =plug; \blacktriangle =slug; \triangle =wavy stratified; \bullet =core-annular; \circ =wavy annular.

E. Pressure Drop Comparison with Prediction Model

Arney et al. [20] developed a non-dimensional pressure drop ϕ ($R = 1/\phi$), based on cylindrical core-annular flow model. From Arney model:

The holdup volume fraction is from an empirical formula [20], $H_w = C_w [1 + 0.35(1 - C_w)]$ (7).

The non-dimensional core diameter η can be used to compute the mixture density ρ_m ,

$$\eta = \sqrt{1 - H_w} \tag{8}$$

$$\rho_m = (1 - \eta^2)\rho_w + \eta^2\rho_o \tag{9}$$

The Reynolds number Re , and friction factor from Blasius formula f , can be expressed as,

$$Re = \frac{D \rho_m J_m}{\mu_o} [1 + \eta^4 \left(\frac{\mu_w}{\mu_o} - 1\right)] \tag{10}$$

$$f = \frac{0.316}{Re^{0.25}} \tag{11}$$

The dimensionless pressure drop is given as:

$$\phi = \frac{D \rho_m J_m^2}{64 \mu_o J_o} f \tag{12}$$

A comparison between the pressure drop reduction factor calculated by Arney et al. [20] [Eqn. (12)] and the present experimental data is shown in Fig.21. From the comparison, there's a good agreement between Arney model and the present experimental data.

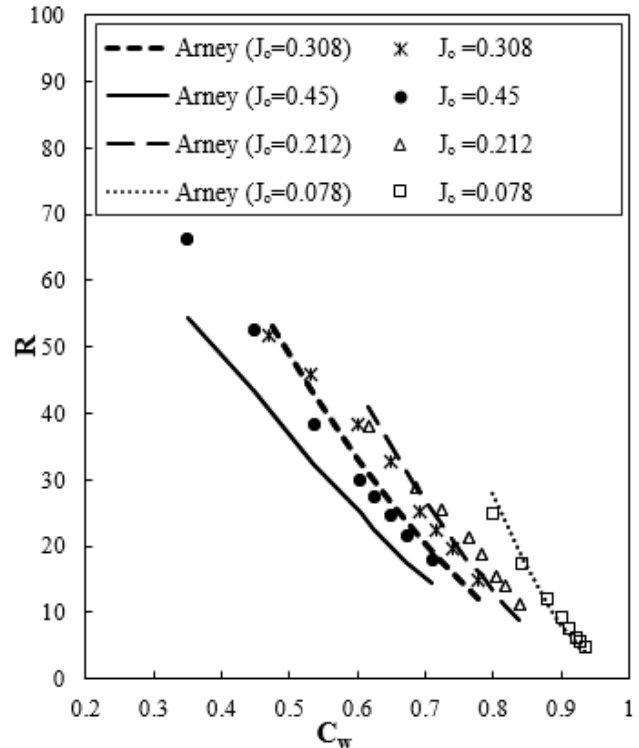


Fig. 21. Pressure drop reduction factor as a function of the water input ratio. Symbols indicate experimental points; different lines represent the Arney's et al. [20] model

VI. ERROR ANALYSIS

The following analysis of the relative error is performed using the relative errors of the measuring instruments in the experimental work. The propagation of errors is calculated using the root sum square method. The result Z is given as a function of the independent variables $x_1, x_2, x_3 \dots x_n$. Generally, in the experimental work, there are two types of errors the first is the measured error and the second is the calculated error.

Let ω_z be the uncertainty in the result and $\omega_{x1}, \omega_{x2}, \omega_{xn}$ be the uncertainties in the independent variables. The uncertainty in the result is calculated according to the following equation:

$$\omega_z = \sqrt{\left(\frac{\partial z}{\partial x_1}\right)^2(\omega_{x1})^2 + \left(\frac{\partial z}{\partial x_2}\right)^2(\omega_{x2})^2 + \dots + \left(\frac{\partial z}{\partial x_n}\right)^2(\omega_{xn})^2} \quad (13)$$

The errors in the measured values such as differential head in U-tube manometer, main pipe diameter, oil viscosity and oil density.

Table 3
Uncertainty in measured values

parameter	Uncertainty
Differential head in U-tube manometer (mm)	± 2 mm
Main pipe diameter (m)	± 0.5 mm
Oil density (kg/m ³)	± 10 g/m ³
mass of oil for certain flow (gram)	± 5 g
Time of oil mass for certain flow (s)	± 5 g
Oil viscosity (mPa.s)	± 50 mPa.s

Table 4
Absolute and Relative errors of the measurement parameters.

Parameter	Absolute Error	Relative Error
Pressure drop (Pa)	19.62	4.78 %
Pressure drop reduction factor, R	4.5	11.96 %
Water flow rate (m ³ /s)	2.825×10^{-6}	1.42 %
Water superficial velocity (m/s)	0.011	3.6 %
Oil flow rate (m ³ /s)	7.09×10^{-6}	7.7 %
oil superficial velocity (m/s)	0.0117	7.95 %

VII. CONCLUSIONS

The effect of varying mean injection water velocity for the same water flow rate of oil-water two-phase flow in a horizontal acrylic pipe on the flow structure and reduction in the pressure drop were experimentally investigated. From the present study, the following conclusions were found:

- For high U_w , dispersed flow has a wide range of operation and the observed CAF has dispersion oil in water at the interface.
- For low U_w , dispersed flow has very limited range and observed CAF is smooth one.
- CAF observed in the three cases at high J_o ($J_o \geq 0.2$ m/s).
- WCAF was found in the three cases at low water input ratio ($C_{w, \min}$).
- The pressure drop reduction factor (R) increases with increasing the oil flow rate (in direction of formation CAF).
- The maximum reduction occurs for high U_w , where the water input ratio decreased to a minimum value without break CAF, so heavy oil can be transferred by using water as a lubricant with a ratio of 30% of total flow rate to achieve reduction in the pressure drop 70 times.
- Experimental data for the measured pressure drop reduction factor were compared with that calculated from the analytical Arney model. From comparison, there is a good agreement between experiments and predictions with error less than 20%.

References

- [1] P. Gateau, I. Hénaut, L. Barré, and J. Argillier, "Heavy oil dilution," *Oil & gas science and technology*, vol. 59, pp. 503-509, 2004.
- [2] B. Toms, "On the early experiments on drag reduction by polymers," *The Physics of Fluids*, vol. 20, pp. S3-S5, 1977.
- [3] A. Saniere, I. Hénaut, and J. Argillier, "Pipeline transportation of heavy oils, a strategic, economic and technological challenge," *Oil & gas science and technology*, vol. 59, pp. 455-466, 2004.
- [4] A. Bensakhria, Y. Peysson, and G. Antonini, "Experimental study of the pipeline lubrication for heavy oil transport," *Oil & gas science and technology*, vol. 59, pp. 523-533, 2004.
- [5] A. Dasari, A. B. Desamala, A. K. Dasmahapatra, and T. K. Mandal, "Experimental studies and probabilistic neural network prediction on flow pattern of viscous oil-water flow through a circular horizontal pipe," *Industrial & Engineering Chemistry Research*, vol. 52, pp. 7975-7985, 2013.
- [6] P. Angeli and G. Hewitt, "Flow structure in horizontal oil-water flow," *International Journal of Multiphase Flow*, vol. 26, pp. 1117-1140, 2000.
- [7] J. Lovick and P. Angeli, "Experimental studies on the dual continuous flow pattern in oil-water flows," *International Journal of Multiphase Flow*, vol. 30, pp. 139-157, 2004.
- [8] A. S. I. Ismail, I. Ismail, M. Zoveidavianpoor, R. Mohsin, A. Piroozian, M. S. Misnan, and M. Z. Sariman, "Experimental investigation of oil-water two-phase flow in horizontal pipes: Pressure losses, liquid holdup and flow patterns," *Journal of Petroleum Science and Engineering*, vol. 127, pp. 409-420, 2015.
- [9] D. H. Vuong, H.-Q. Zhang, C. Sarica, and M. Li, "Experimental study on high viscosity oil/water flow in horizontal and vertical pipes," in *SPE annual technical conference and exhibition*, 2009.
- [10] G. Sotgia, P. Tartarini, and E. Stalio, "Experimental analysis of flow regimes and pressure drop reduction in oil-water mixtures," *International Journal of Multiphase Flow*, vol. 34, pp. 1161-1174, 2008/12/01/ 2008.
- [11] P. Poesio, D. Strazza, and G. Sotgia, "Two-and three-phase mixtures of highly-viscous-oil/water/air in a 50 mm id pipe," *Applied Thermal Engineering*, vol. 49, pp. 41-47, 2012.
- [12] B. Grassi, D. Strazza, and P. Poesio, "Experimental validation of theoretical models in two-phase high-viscosity ratio liquid-liquid flows in horizontal and slightly inclined pipes," *International Journal of Multiphase Flow*, vol. 34, pp. 950-965, 2008.
- [13] P. Hanafizadeh, A. Hojati, and A. Karimi, "Experimental investigation of oil-water two phase flow regime in an inclined pipe," *Journal of Petroleum Science and Engineering*, vol. 136, pp. 12-22, 2015/12/01/ 2015.
- [14] M. E. Charles, G. t. Govier, and G. Hodgson, "The horizontal pipeline flow of equal density oil-water mixtures," *the Canadian Journal of Chemical engineering*, vol. 39, pp. 27-36, 1961.
- [15] T. Fujii, J. Ohta, T. Nakazawa, and O. Morimoto, "The behavior of an immiscible equal-density liquid-liquid two-phase flow in a horizontal tube," *JSME International Journal Series B Fluids and Thermal Engineering*, vol. 37, pp. 22-29, 1994.
- [16] S. Abraham and A. F. Clark, "Method of pumping viscous petroleum," ed: Google Patents, 1950.
- [17] G. Ooms, A. Segal, A. Van Der Wees, R. Meerhoff, and R. Oliemans, "A theoretical model for core-annular flow of a very viscous oil core and a water annulus through a horizontal pipe," *International Journal of Multiphase Flow*, vol. 10, pp. 41-60, 1983.
- [18] R. Miesen, G. Beijnon, P. Duijvestijn, R. Oliemans, and T. Verheggen, "Interfacial waves in core-annular flow," *Journal of fluid mechanics*, vol. 238, pp. 97-117, 1992.
- [19] R. V. A. Oliemans, G. Ooms, H. L. Wu, and A. Duijvestijn, "Core-annular oil/water flow: the turbulent-lubricating-film model and measurements in a 5 cm pipe loop," *International Journal of Multiphase Flow*, vol. 13, pp. 23-31, 1987/01/01/ 1987.
- [20] M. S. Arney, R. Bai, E. Guevara, D. D. Joseph, and K. Liu, "Friction factor and holdup studies for lubricated pipelining—I. Experiments and correlations," *International Journal of Multiphase Flow*, vol. 19, pp. 1061-1076, 1993/12/01/ 1993.
- [21] A. Beretta, P. Ferrari, L. Galbiati, and P. Andreini, "Horizontal oil-water flow in small diameter tubes. Pressure drop," *International communications in heat and mass transfer*, vol. 24, pp. 231-239, 1997.
- [22] N. Brauner and A. Ullmann, "Modeling of phase inversion phenomenon in two-phase pipe flows," *International Journal of Multiphase Flow*, vol. 28, pp. 1177-1204, 2002.

- [23] N. Brauner, "Two-phase liquid-liquid annular flow," *International Journal of Multiphase Flow*, vol. 17, pp. 59-76, 1991.
- [24] W. L. Loh and V. K. Premanadhan, "Experimental investigation of viscous oil-water flows in pipeline," *Journal of Petroleum Science and Engineering*, vol. 147, pp. 87-97, 2016/11/01/ 2016.
- [25] X. Luo, G. Lü, W. Zhang, L. He, and Y. Lü, "Flow structure and pressure gradient of extra heavy crude oil-water two-phase flow," *Experimental Thermal and Fluid Science*, vol. 82, pp. 174-181, 2017/04/01/ 2017.
- [26] A. Huang, C. Christodoulou, and D. D. Joseph, "Friction factor and holdup studies for lubricated pipelining—II Laminar and $\kappa\epsilon$ models of eccentric core flow," *International Journal of Multiphase Flow*, vol. 20, pp. 481-491, 1994.
- [27] J. Rovinsky, N. Brauner, and D. M. Maron, "Analytical solution for laminar two-phase flow in a fully eccentric core-annular configuration," *International Journal of Multiphase Flow*, vol. 23, pp. 523-543, 1997.
- [28] T. Ko, H. Choi, R. Bai, and D. Joseph, "Finite element method simulation of turbulent wavy core-annular flows Using a $k-\omega$ Turbulence Model Method," *International Journal of Multiphase Flow*, vol. 28, pp. 1205-1222, 2002.
- [29] E. M. R. M. Ingen Housz, G. Ooms, R. A. W. M. Henkes, M. J. B. M. Pourquie, A. Kidess, and R. Radhakrishnan, "A comparison between numerical predictions and experimental results for horizontal core-annular flow with a turbulent annulus," *International Journal of Multiphase Flow*, vol. 95, pp. 271-282, 2017/10/01/ 2017.
- [30] J. Shi, M. Gourma, and H. Yeung, "CFD simulation of horizontal oil-water flow with matched density and medium viscosity ratio in different flow regimes," *Journal of Petroleum Science and Engineering*, vol. 151, pp. 373-383, 2017/03/01/ 2017.